

We are IntechOpen, the world's leading publisher of Open Access books Built by scientists, for scientists

6,900

Open access books available

186,000

International authors and editors

200M

Downloads

Our authors are among the

154

Countries delivered to

TOP 1%

most cited scientists

12.2%

Contributors from top 500 universities



WEB OF SCIENCE™

Selection of our books indexed in the Book Citation Index
in Web of Science™ Core Collection (BKCI)

Interested in publishing with us?
Contact book.department@intechopen.com

Numbers displayed above are based on latest data collected.
For more information visit www.intechopen.com



Analytical Model for Seal Contact Pressure

Sayyad Zahid Qamar, Maaz Akhtar and Tasneem Pervez

*As far as the laws of mathematics refer to reality, they are not certain;
and as far as they are certain, they do not refer to reality.*

Albert Einstein

Abstract

Swellable elastomers are used for zonal isolation and as an alternate to cementing is a new approach, resulting in significant reduction in time, cost, and weight. Very large strains, flexibility, resilience, and durability are their special features. Performance analysis is important design improvement and appropriate selection of swell packers. Experimental evaluation of swelling-elastomer seal performance can be very costly, and is not even possible in many cases. Numerical simulations (Chapters 8 and 9) can be more convenient, but computational effort and cost can be high. Development of closed-form (analytical) solutions is presented in this chapter to estimate the variation of contact pressure along the length of the elastomer seal. Major relevant parameters are properties of the material elastomer, seal configuration and size, magnitude of seal compression, and differential pressure across the seal. Numerical (finite element) modeling and simulation is also performed. There was good conformity between analytical and simulation results, validating the soundness of the analytical solution, and providing assurance that it can reliably predict the sealing response of the elastomer. A comprehensive parametric study is then conducted to assess seal performance while varying different key factors. Properties of the elastomer material (as it swells with exposure time) are required to run the analytical and the FE models. A large set of experiments were therefore designed and conducted to evaluate mechanical properties (E , G , K , and ν) of the elastomer with gradual swelling (Chapters 3 and 7).

Keywords: Swelling elastomers, seal contact pressure, contact friction, analytical model

1. Introduction

In petroleum drilling and development, cementing is an established method used to hydraulically seal the steel casing from the rock formation (open hole), or the inside casing from the outside casing (closed hole). It serves the function of isolating certain zones and of preventing flow in the annular region [1]. Design and implementation of a cement job is a complex process, and many factors must be considered for its successful completion. Using swellable elastomers as a full or partial alternate to cementing is a new approach, resulting in significant reduction

in time, cost, and weight [2]. Elastomers can withstand very large strains without any permanent deformation [3]. Flexibility, extensibility, resilience, and durability are the special additional features that elastomers offer [4, 5]. Without some sort of performance analysis, one cannot proceed with appropriate selection of a swell packer for a given set of field conditions, improvement of sealing design, assessment of seal integrity, etc. [6–8].

Main motivation for this work is the need for performance evaluation of swelling (and inert) elastomer seals used in petroleum applications. Experimental evaluation of swelling-elastomer seal performance can be very costly, and is not even possible in many cases [9]. Numerical simulations (Chapters 8 and 9), if validated, can be more convenient, but computational effort and cost can be high as simulations have to be run for each set of conditions [10, 11]. A well-founded analytical approach not only gives an elegant closed-form solution, but can give reasonably accurate and much faster prediction of elastomer performance under various actual oil and gas field conditions [12].

Development of closed-form (analytical) solutions is presented in this chapter to estimate the variation of contact pressure along the length of the elastomer seal. Major relevant parameters are properties of the material elastomer, seal configuration and size, magnitude of seal compression, and differential pressure across the seal [13]. Numerical (finite element) modeling and simulation is also performed. There was good conformity between analytical and simulation results, validating the soundness of the analytical solution, and providing assurance that it can reliably predict the sealing response of the elastomer. A comprehensive parametric study is then conducted to assess seal performance while varying different key factors. Properties of the elastomer material (as it swells with exposure time) are required to run the analytical and the FE models. A large set of experiments were therefore designed and conducted to evaluate mechanical properties (E , G , K , and ν) of the elastomer with gradual swelling (Chapters 3 and 7).

2. Rubber block under compressive loading

Various researchers have studied how an elastic rubber block behaves when subjected to transverse loading. Typically, a rubber block is in contact with two rigid plates, one above it, and one below it; **Figure 1**. Contact between the plates and the rubber block is full bonding or friction type [14, 15]. There will be a symmetric bulge in the central region of the rubber block if there is perfect bonding on both sides, or if the friction coefficient (sliding) on both contacting surfaces is the same. Bulging will be asymmetric otherwise. If friction is higher, amount of sliding will of course be lower. In the ideal case of frictionless contact (zero coefficient of friction), sliding will be maximum. In the extreme opposite case of bonded contact (infinite coefficient of friction), there will be no sliding. Published studies consistently show that the behavior is significantly different for rigid plates bonded above and below to an elastic layer, as compared with unbonded elastic layer [16, 17].

Majority of previous reports are based on the assumption that the strains are very small, so that problem can be modeled as a linear one. Some studies allow a little variation in friction at the contact surface, the treatment being somewhat closer to the actual case of elastomer seals in swellable packers. However, all these models have the symmetrical condition of full bonding or frictional contact on both sides. The few studies that address the more realistic case of bonding on one side and frictional contact on the other, treat the rubber material as incompressible, adopt an energy approach, and use a linear elastic model based on only the elastic modulus (E) of the seal material.

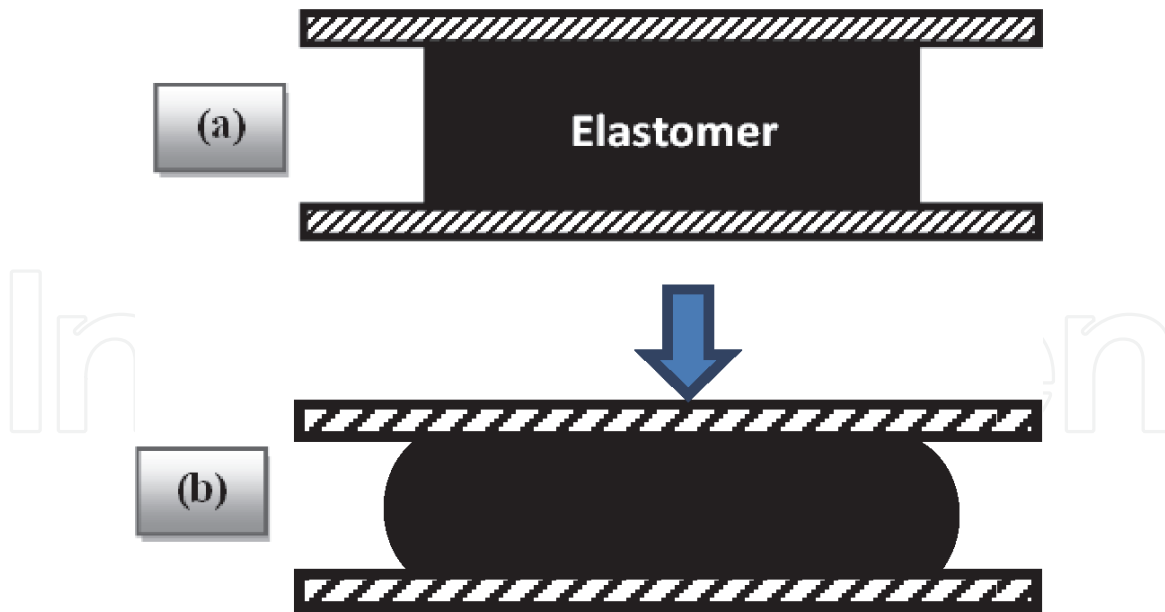


Figure 1.
 Schematic diagram of deformation of elastic rubber block under transverse compressive loading; (a) before loading; (b) after loading.

2.1 Current work

None of the published studies faithfully represent the real case of inert or swelling elastomer packers used in petroleum engineering. The representative salient features that differentiate the current approach (this chapter) from all of the earlier studies are listed below.

- a. Elastomer material is considered as compressible, a major shift in comparison with all earlier studies based on incompressibility (single value of Poisson's ratio: 0.5).
- b. Rather than the simple geometry of flat plates, elastomer seal has a cylindrical contact on both sides, as in the real downhole situation of elastomer mounted on a steel tubular and sealing against an outer steel casing or rock formation.
- c. On one side, the elastomer is fully bonded (inner steel pipe), while on the other side it has frictional contact (with outer steel casing or formation).
- d. A volume-change approach is used in contrast to the typical energy-method.
- e. A more robust and realistic model is used, incorporating both elastic and bulk behavior of the elastomer material (E and K).

All of the above more realistic conditions form the basis of a closed form analytical model to describe the behavior of elastomer seals in the form of contact pressure variation along the seal length, when the seal is subjected to differential fluid pressure. Numerical modeling and simulation of the same problem is also carried out. Conducting experiments on actual swell packers under a variety of oil well conditions is time and cost wise prohibitive, if not practically impossible. Good agreement between the two approaches therefore serves as a good form of validation of the analytical model. A parametric study is then conducted to assess

how seal performance is affected by changes in seal design parameters and well conditions (seal geometry, seal compression, differential pressure, and elastomer material) on.

3. Analytical model

When a swell packer comes in contact with a swelling medium (generally water or oil), the elastomer swells primarily in the radial direction. The annular gap is sealed when the elastomer touches the outer casing (or formation). As the rubber swells further, more and more compressive force is generated against the outer casing, causing sealing pressure to increase; **Figure 2**. Normal contact stress is a function of friction at the contact surface. To derive a closed form solution for sealing pressure, a step-wise approach is used. For the initial case of fully bonded contact, the friction coefficient (μ) approaches infinity, resulting in no sliding. In a real well, this can happen when roughness of the rock formation is high enough to prevent sliding. The second scenario is the extreme opposite case of free-sliding contact (zero friction). These two extreme conditions form the basis for the seal pressure model for the more complex but realistic case of frictional contact.

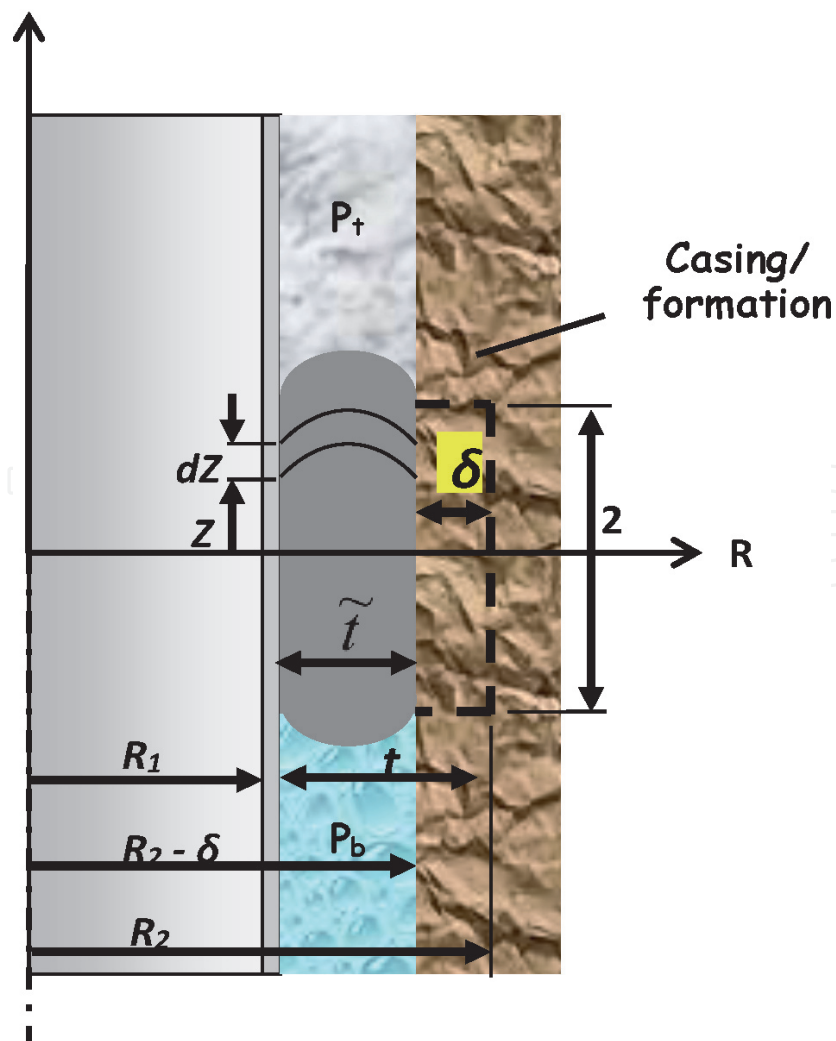


Figure 2.
Geometrical parameters of elastomer seal.

Some of the more fundamental assumptions, closely representing the case of swelling elastomer seals in petroleum drilling operations, are listed below.

- a. Elastomer material is homogenous, isotropic, and linear elastic.
- b. After deformation, the rubber seal takes on a parabolic shape. In the analytical models developed by Gent and Lindley [16], and Yeoh et al. [17], it is shown that the deformed shape (under compression) does become parabolic.
- c. Compression along the circumference of the elastomer seal is uniform. This is necessary to get a valid approximate solution.
- d. There is perfect bonding between the steel tubular and the elastomer segment.
- e. Friction at the contact surface between the elastomer and the outer casing (or rock formation) follows Coulomb's law.

3.1 Case-1: bonded contact

Forces on an elastomer element, and the change in geometry of this element are shown in **Figure 3**, where h is half seal length, Z is location of differential element along seal axis, dZ is length of differential element, p_t is fluid pressure above the seal (top region), and p_b is fluid pressure below the seal (bottom region). General equation of deformed shape of the seal in the case of the bonded (non-sliding) contact is

$$w(R,Z) = -\frac{4q(Z)}{\tilde{t}^2} \left[(R - R_1)^2 - \tilde{t}(R - R_1) \right], \tag{1}$$

where R is seal radius, Z is location of differential element along seal axis, t is seal thickness, R_1 is inner radius of the seal, \tilde{t} is compressed seal thickness, and $q(Z)$ represents the maximum deflection of the compressed seal in the Z -direction. From basic mechanics, the general stress-strain relationships in cylindrical coordinate system are [18].

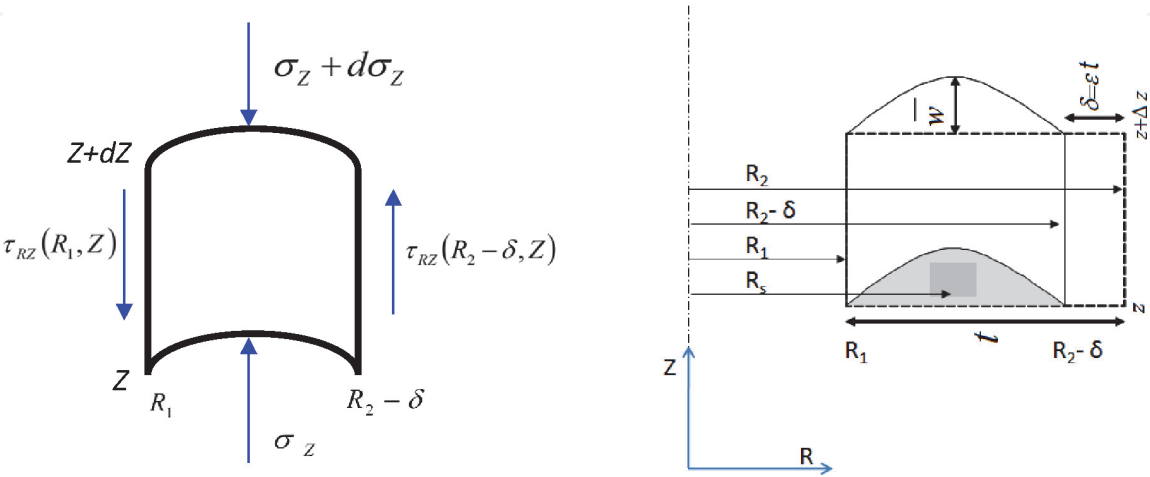


Figure 3.
Forces on an elastomer element (left), and geometry of the volume change element (right).

$$\begin{aligned}
\varepsilon_R &= \frac{\delta}{t} \quad (\text{a}), \\
\varepsilon_Z &= \frac{\partial w}{\partial Z} = -\frac{4}{\tilde{t}^2} \frac{\partial q(Z)}{\partial Z} \left[(R - R_1)^2 - \tilde{t}(R - R_1) \right] \quad (\text{b}), \\
\gamma_{RZ} &= \frac{\partial w}{\partial R} = -\frac{4q(Z)}{\tilde{t}^2} [2(R - R_1) - \tilde{t}] \quad (\text{c}) \\
\sigma_R &= \frac{E}{(1 + \nu)} \varepsilon_R + \frac{3\nu}{(1 + \nu)} p, \quad (\text{d}) \\
\sigma_Z &= \frac{E}{(1 + \nu)} \varepsilon_Z + \frac{3\nu}{(1 + \nu)} p, \quad (\text{e}) \\
\tau_{RZ} &= G\gamma_{RZ} = -\frac{4Gq(Z)}{\tilde{t}^2} [2(R - R_1) - \tilde{t}] \quad (\text{f})
\end{aligned} \tag{2}$$

Here, ε_R , ε_Z , γ_{RZ} , σ_R , σ_Z , and τ_{RZ} are the radial, longitudinal and shear components of strain and stress and respectively, while p is the hydrostatic pressure on the seal ends, and δ is the amount of seal compression. Also, E , K , ν , and G are the elastic modulus, bulk modulus, Poisson's ratio, and shear modulus of the elastomeric material respectively. This set of equations (a to f) will be referred to as Eq. (2). The main objective of the new model is to find the stress in the radial direction (σ_R), which is the sealing pressure created by rubber swelling against outer tubular or formation.

We now apply static force equilibrium ($\sum F_Z = 0$) on the small axi-symmetric elastomer element described in **Figure 3**.

$$\begin{aligned}
&\pi \left[(R_2 - \delta)^2 - R_1^2 \right] \int_{R_1}^{R_2 - \delta} (\sigma_Z + d\sigma_Z - \sigma_Z) dR \\
&+ 2\pi R_1 dZ \tau_{RZ}(R_1, Z) - 2\pi (R_2 - \delta) dZ \tau_{RZ}(R_2 - \delta, Z) = 0
\end{aligned} \tag{3}$$

Here, R_2 is the outer radius of the seal after swelling.

Considering seal length to be much larger than its thickness ($H \gg t$), a very realistic assumption, and simplifying, we get

$$\frac{dp}{dZ} + \left(\frac{4Eq(Z)}{3\nu\tilde{t}^3} \right) = 0. \tag{4}$$

Determination of $q(Z)$ is first required to evaluate the pressure $p(Z)$. Using the standard bulk modulus relationship $\Delta V/V_i = -p/K$ as the starting point, we consider the initial volume (V_i) and the change in volume (ΔV) of the differential element, and allow $\Delta Z \rightarrow 0$. As we know that $R_s = R_1 + (1/2)\tilde{t}$, we can obtain.

$$\frac{dq(Z)}{dZ} = \frac{3R_2\delta}{2R_s\tilde{t}} - \frac{3t(R_2 + R_1)}{4R_s\tilde{t}K} p(Z) \tag{5}$$

Eq. (4) now becomes

$$\frac{d^2 p}{dZ^2} - \lambda_1^2 p(Z) = -\alpha_1, \tag{6}$$

where $\lambda_1^2 = \left(\frac{t(R_2 + R_1)E}{\nu\tilde{t}^4 R_s K} \right)$ and $\alpha_1 = \frac{2R_2\delta E}{\nu\tilde{t}^4 R_s}$.

Solving the above differential equation, we get

$$p(Z) = A \sinh(\lambda_1 Z) + B \cosh(\lambda_1 Z) + \alpha_1 / \lambda_1^2. \quad (7)$$

A and B are arbitrary constants determined from boundary conditions. Application of the boundary conditions [$p(Z = h) = p_t$ and $p(Z = -h) = p_b$] and simplification results in the following relations for pressure distribution and normal contact stress in the non-sliding (NS) case:

$$p(Z) = \left(\frac{p_t - p_b}{2 \sinh(\lambda_1 h)} \right) \sinh(\lambda_1 Z) + \left(\frac{p_t + p_b - \frac{2\alpha_1}{\lambda_1^2}}{2 \cosh(\lambda_1 h)} \right) \cosh(\lambda_1 Z) + \frac{\alpha_1}{\lambda_1^2} \quad (8)$$

$$\sigma_{R_NS}(Z) = \frac{E}{(1+\nu)} \frac{\delta}{t} + \frac{3\nu}{(1+\nu)} * \left(\left(\frac{p_t - p_b}{2 \sinh(\lambda_1 h)} \right) \sinh(\lambda_1 Z) + \left(\frac{p_t + p_b - \frac{2\alpha_1}{\lambda_1^2}}{2 \cosh(\lambda_1 h)} \right) \cosh(\lambda_1 Z) + \frac{\alpha_1}{\lambda_1^2} \right). \quad (9)$$

3.2 Case-2: free sliding

A mirror opposite of the first one, the second case represents free sliding or frictionless contact at the elastomer-formation boundary. This translates into zero shear strain (and shear stress) at the contact surface. We again start with force equilibrium, follow a similar series of steps, and use the substitution $R_s = R_1 + (5/8)\tilde{t}$ in Eq. (5) to get.

$$\frac{d^2 p}{dZ^2} - \lambda_2^2 p(Z) = -\alpha_2 \quad (10)$$

In the above equation,

$$\lambda_2^2 = \left(\frac{R_1 t (R_2 + R_1) E}{2\nu(R_2 - \delta + R_1) R_s \tilde{t}^4 K} \right), \text{ and } \alpha_2 = \frac{R_1 R_2 \delta E}{\nu(R_2 - \delta + R_1) R_s \tilde{t}^4}.$$

Further simplification yields the contact pressure and normal stress distribution for the free sliding (S) case:

$$p(Z) = \left(\frac{p_t - p_b}{2 \sinh(\lambda_2 h)} \right) \sinh(\lambda_2 Z) + \left(\frac{p_t + p_b - \frac{2\alpha_2}{\lambda_2^2}}{2 \cosh(\lambda_2 h)} \right) \cosh(\lambda_2 Z) + \frac{\alpha_2}{\lambda_2^2} \quad (11)$$

$$\sigma_{R_S}(Z) = \frac{E}{(1+v)} \frac{\delta}{t} + \frac{3v}{(1+v)} * \left(\left(\frac{p_t - p_b}{2 \sinh(\lambda_2 h)} \right) \sinh(\lambda_2 Z) + \left(\frac{p_t + p_b - \frac{2\alpha_2}{\lambda_2^2}}{2 \cosh(\lambda_2 h)} \right) \cosh(\lambda_2 Z) + \frac{\alpha_2}{\lambda_2^2} \right). \quad (12)$$

3.3 Case-3: frictional contact

The last and final case is the more realistic one of frictional contact at the elastomer-formation boundary; somewhere in between the two extreme cases of bonded contact and free-sliding. Frictional contact is defined at a cylindrical surface rather than a flat surface. If the rubber is vulcanized to the inner casing (fully bonded on one side), and contact on the other side (formation or outer casing) is frictional in nature, there will be a non-symmetrical bulging in the middle. Its magnitude is dictated by friction at outer contact surface; as friction coefficient (μ) increases, the amount of sliding decreases. To derive the normal contact stress distribution, we consider a weighted sum of the two extreme cases described above.

$$\sigma_{R_F}(Z) = (1 - \mu)[\sigma_{R_S}(Z)] + (\mu)[\sigma_{R_{NS}}(Z)] \quad (13)$$

Expanded form of this equation is shown below.

$$\sigma_{R_F}(Z) = \left(\left[\left(\frac{p_t - p_b}{2 \sinh(\lambda_2 h)} \right) \sinh(\lambda_2 Z) + \left(\frac{p_t + p_b - \frac{2\alpha_2}{\lambda_2^2}}{2 \cosh(\lambda_2 h)} \right) \cosh(\lambda_2 Z) + \frac{\alpha_2}{\lambda_2^2} \right] - \frac{3v\mu}{(1+v)} \left[\left(\frac{p_t - p_b}{2 \sinh(\lambda_1 h)} \right) \sinh(\lambda_1 Z) + \left(\frac{p_t + p_b - \frac{2\alpha_1}{\lambda_1^2}}{2 \cosh(\lambda_1 h)} \right) \cosh(\lambda_1 Z) + \frac{\alpha_1}{\lambda_1^2} \right] \right). \quad (14)$$

Figure 4 shows the variation of contact pressure along the seal length for the three cases, described by this last Eq. (14). Making intuitive sense, pressure curve for this frictional contact lies between the previous two extreme cases of full bonding and free sliding. Also, higher friction generates higher sealing pressure. As can be seen in **Figure 4**, location of maximum pressure is at the seal center. This value can be determined by putting $Z = 0$ in Eq. (14), yielding the following equation.

$$\sigma_{R_F}(Z = 0) = \left(\left[\left(\frac{p_t + p_b - \frac{2\alpha_2}{\lambda_2^2}}{2 \cosh(\lambda_2 h)} \right) + \frac{\alpha_2}{\lambda_2^2} \right] - \frac{3v\mu}{(1+v)} \left[\left(\frac{p_t + p_b - \frac{2\alpha_1}{\lambda_1^2}}{2 \cosh(\lambda_1 h)} \right) + \frac{\alpha_1}{\lambda_1^2} \right] \right) \quad (15)$$

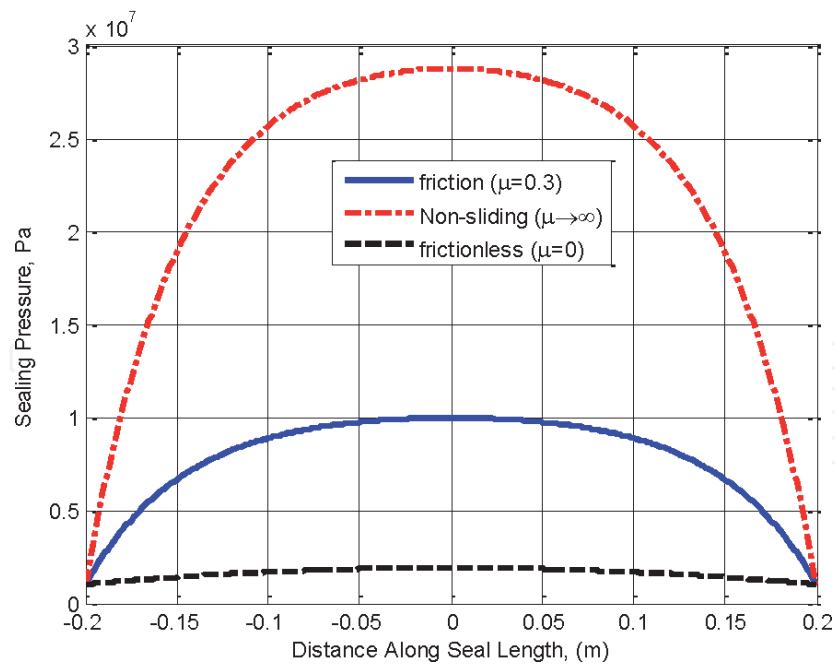


Figure 4.
Normal contact stress distribution along the elastomer seal for the three cases (sliding, no-sliding, frictional); $E = 0.20 \text{ MPa}$, $p_t = 1 \text{ MPa}$, $p_b = 1 \text{ MPa}$, $t = 20 \text{ mm}$, $H = 400 \text{ mm}$, $R_1 = 100.33 \text{ mm}$, $\delta = 1 \text{ mm}$.

4. Numerical model

Numerical modeling and simulation of swelling-elastomer seal has been done here using the commercial finite element analysis (FEA) package ABAQUS. An axisymmetric model was deemed sufficient as both loads and geometry are

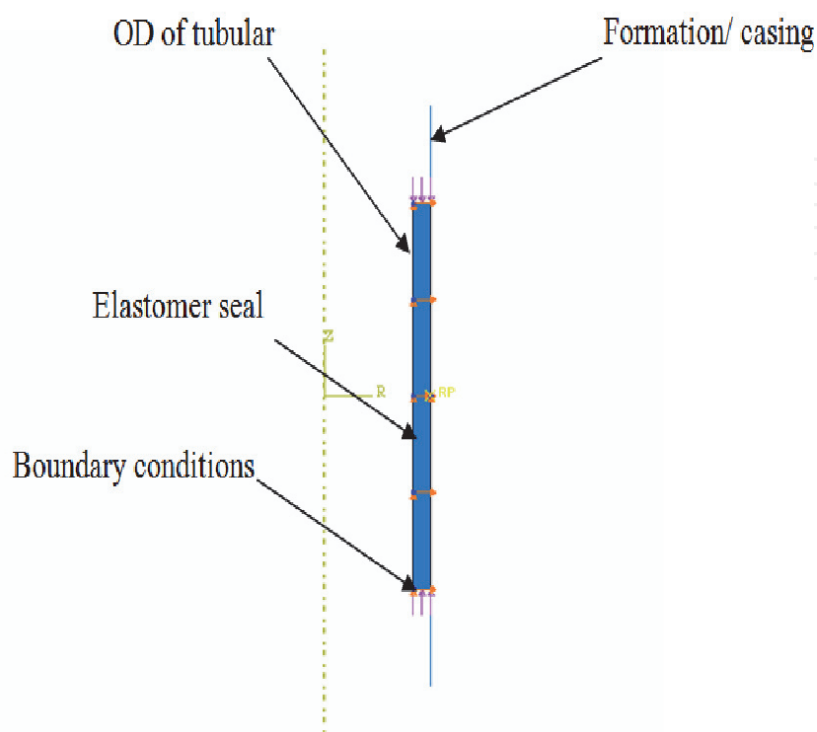


Figure 5.
Finite element model showing the elastomer seal and boundary conditions.

symmetric. The rubber element is treated as a deformable material, and in comparison the outer casing or formation is treated as a rigid body. Using an actual regional oilfield as a base, numerical model was developed for a seal length (H) of 400 mm; a steel tubular having an outer radius of (R_1) of 100.33 mm, same as the seal inner radius; and an elastomer seal having a thickness (t) of 20 mm. By using a Poisson's ratio (ν) value of 0.4999, the seal material was rendered almost incompressible for bulk deformation. The neo-Hookean hyperelastic material model was used to represent the elastomer material. Actual data sets from compression experiments conducted on laboratory size elastomer samples at various swelling intervals were used to extract the model coefficients. **Figure 5** is a depiction of the FE model with axisymmetric boundary conditions, while **Figure 6** shows the simulation results for variation of sealing pressure along the length of the seal.

Analytical and FEA results for seal pressure variation over the seal length are compared against each other in **Figure 7** for two values of μ . Simulated and theoretical results were plotted for many other conditions also, but are not shown here due to space limitation. All the comparative graphs exhibit a close agreement

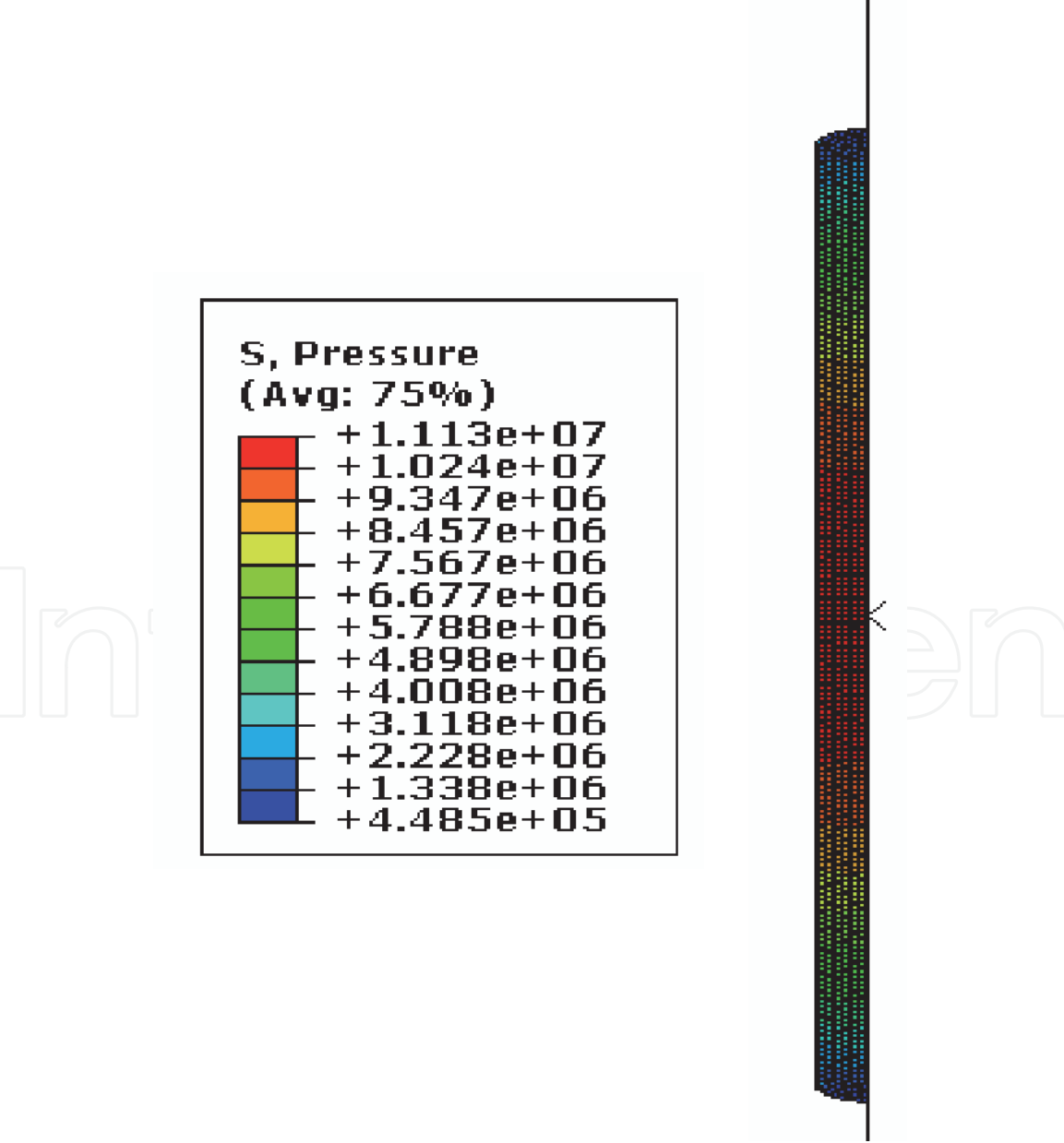


Figure 6.
Finite element simulation of variation of sealing pressure along the elastomer seal.

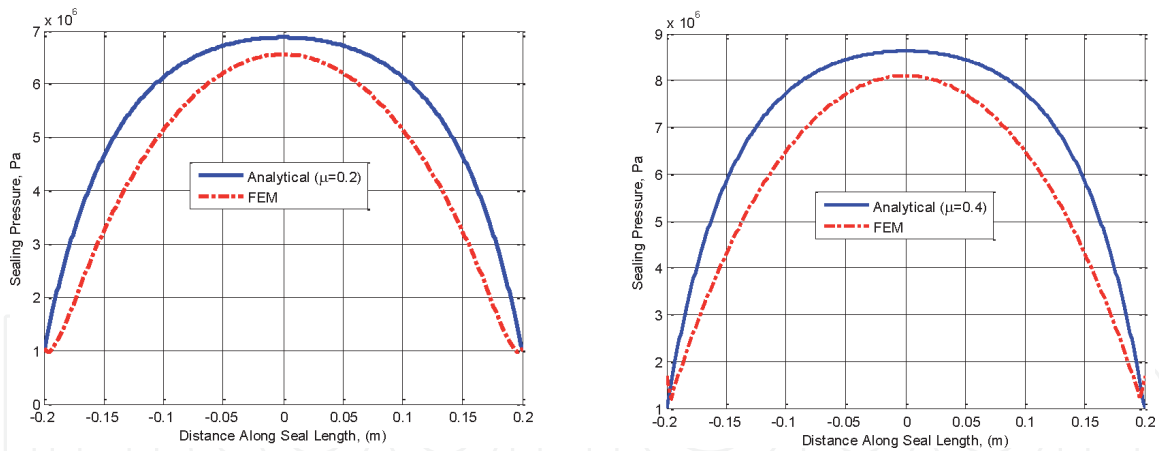


Figure 7. Comparison of analytical and numerical results for sealing pressure distribution for $\mu = 0.2$ (left) and $\mu = 0.4$ (right); $E = 0.20$ MPa, $p_t = 1$ MPa, $p_b = 1$ MPa, $t_i = 20$ mm, $H = 400$ mm, $R_1 = 100.33$ mm, $\delta = 1$ mm.

between FE and analytical results. However, it is noteworthy that the analytical model gives a slightly higher sealing pressure than the FE model in all cases. A probable explanation is that the numerical model also includes material nonlinearity (neo-Hookean hyperelastic material model), while the analytical model considers the rubber to be a linear elastic material.

5. Results and discussion

The last Eq. (15) describes the contact pressure generated by the elastomer seal as a function of seal compression, seal length, seal thickness, and elastomer material properties. Given below is a parametric study of how the maximum sealing pressure behaves as different seal parameters are varied.

Maximum contact pressure (p_{max}) is plotted as a function of seal length (H) for different values of seal compression (δ) in **Figure 8**. Sealing pressure distribution along the seal is not constant but varies nonlinearly depending on seal parameters and loading conditions, with maximum sealing pressure occurring at the center of the seal length. In all cases, there is an initial sharp increase in sealing pressure for increasing seal length, which gradually becomes almost constant once the seal length crosses a value of 40 cm. This observation has a major practical and economic bearing for field engineers. ***A seal length of more than 40 cm is impractical; it will not generate higher seal pressure. Limiting length of individual rubber elements to 40 cm can result in major cost and weight savings.*** To be practically more effective, several 40-cm seal elements can be mounted in series for more effective zonal isolation.

It can be observed from **Figure 8** that larger amount of seal compression produces higher pressure curves. Again, this is as expected; more compression generates higher sealing pressure. Elastomer can be compressed by a larger amount by using a material that swells more under the given conditions, or by using swell packers together with solid expandable tubular (SET) technology. In an SET application, a petroleum tubular (with elastomer seal mounted on it) is expanded downhole by forcing a conical mandrel through it, thus blocking the perforations and shutting off an unwanted zone.

Variation of maximum seal pressure as a function of seal length can be seen in **Figure 9** for different values of seal thickness. The apparently counter-intuitive observation, that sealing pressure decreases with increasing seal thickness, needs a little explanation. As explained earlier in Chapter-7, this happens because seal

pressurization is modeled here (numerically) in the form of a fixed amount of displacement, while seal thickness is changed. At the beginning, the elastomer seal is just touching the casing wall. As the displacement (δ) is now applied, the elastomer undergoes compression. If the seal is thin, the compression ratio (δ divided by seal thickness t) is much larger, thus the behavior seen in **Figure 9**. It is therefore better to use the term “compression ratio” rather than “seal compression.” Sealing pressure increases (almost proportionately) as compression ratio is increased, as expected; **Figure 10**.

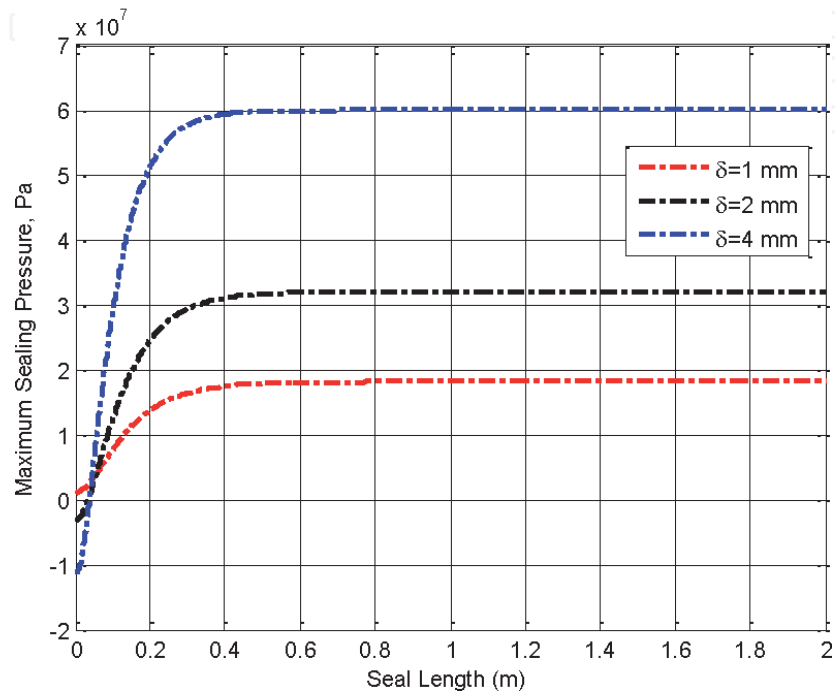


Figure 8.
Maximum seal pressure as a function of seal length for different values of seal compression; $E = 0.33 \text{ MPa}$, $p_t = 1 \text{ MPa}$, $p_b = 0 \text{ MPa}$, $t = 20 \text{ mm}$.

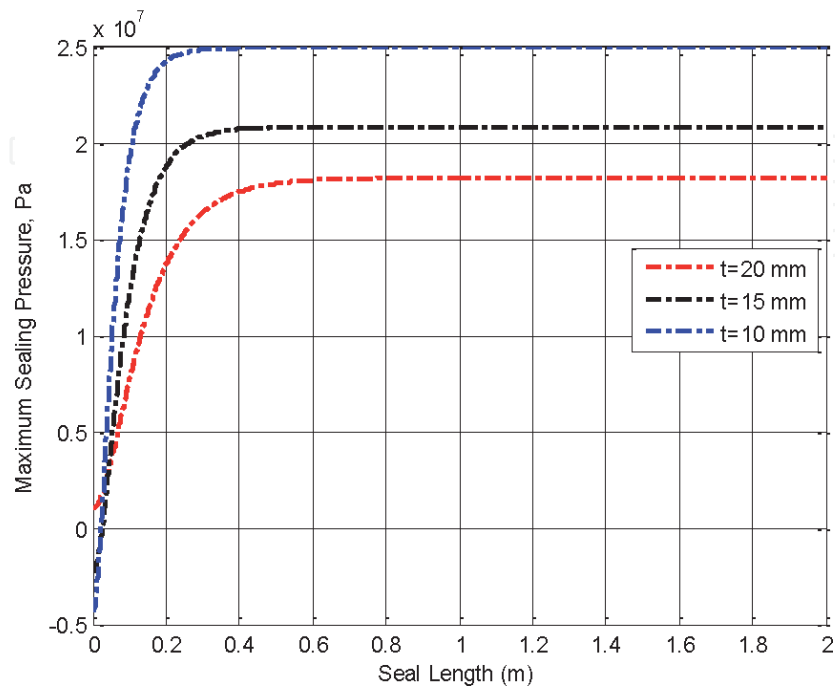


Figure 9.
Maximum seal pressure as a function of seal length for different values of seal thickness; $E = 0.33 \text{ MPa}$, $p_t = 1 \text{ MPa}$, $p_b = 0 \text{ MPa}$, $H = 400 \text{ mm}$, $R_1 = 100.33 \text{ mm}$, $\mu = 0.2$.

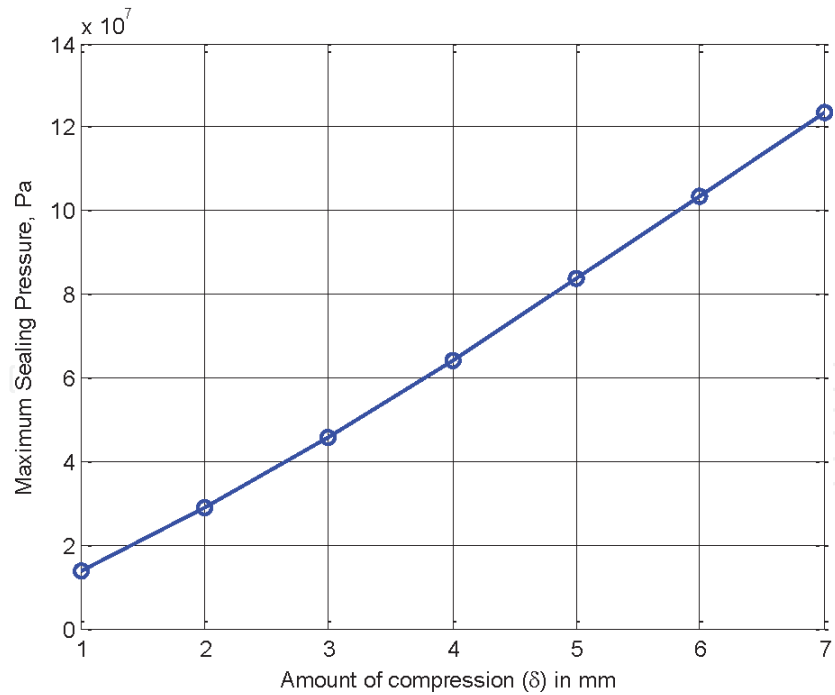


Figure 10.
Maximum sealing pressure is directly proportional to seal compression for constant seal thickness;
 $E = 0.33 \text{ MPa}$, $p_t = 1 \text{ MPa}$, $p_b = 0 \text{ MPa}$, $t = 20 \text{ mm}$, $H = 400 \text{ mm}$, $R_1 = 100.33 \text{ mm}$, and $\mu = 0.2$.

6. Conclusions

An analytical (mathematical) model has been developed to quantify the pressure distribution along an elastomer seal as a function of seal geometry (thickness, length, etc.), material properties of rubber and steel pipe (E , G , K , and ν), friction at the contact surface, and differential pressure across the seal in an oil well. This approach of using actual swelling elastomer seals and packers as a base makes this model significantly different from previous studies. On the inner side, the elastomer is bonded (vulcanized) to a petroleum tubular, and on the outer side it has a frictional contact with an outer casing or rock formation. Instead of considering only the elastic modulus of the material, the model uses both E and K values of the elastomer material. Rather than assuming the elastomer to be incompressible, the value of Poisson's ratio is taken to be different from 0.5. As opposed to the conventional energy-method, a volume-change approach is adopted.

The problem is also modeled and simulated numerically. Results from numerical simulations and analytical model are quite close to each other, confirming that the mathematical model gives good prediction of sealing behavior of the elastomer. Variation of sealing pressure along the seal is nonlinearly in nature, and depends on seal parameters and well conditions. It reaches a maximum value at the center of the seal. Very longer seals are impractical; after a seal length of 40 cm, sealing pressure does not increase much. Larger compression ratio generates higher sealing pressure. More seal compression can be achieved by using an elastomer that swells more, or by using swelling elastomers together with SET expansion. If the applied seal compression is kept constant, thinner seal yields higher compression ratio; this generates higher sealing pressure.

This analytical model is a major improvement on previous models, saves a lot of computational time in comparison with numerical models, and gives reasonably accurate prediction of elastomer seal performance under various actual oil and gas field conditions. The obtained results are of major interest for academics and researchers, petroleum engineers, and swell packer designers and manufacturers.

IntechOpen

Author details


Sayyad Zahid Qamar^{1*}, Maaz Akhtar² and Tasneem Pervez¹

1 Mechanical and Industrial Engineering Department, Sultan Qaboos University, Muscat, Oman

2 Mechanical Engineering Department, N.E.D. University of Engineering and Technology, Karachi, Pakistan

*Address all correspondence to: sayyad@squ.edu.om

IntechOpen

© 2021 The Author(s). Licensee IntechOpen. Distributed under the terms of the Creative Commons Attribution - NonCommercial 4.0 License (<https://creativecommons.org/licenses/by-nc/4.0/>), which permits use, distribution and reproduction for non-commercial purposes, provided the original is properly cited. 

References

- [1] Bellarby J (2009), Well Completion Design, Elsevier
- [2] Kennedy G, Lawless A, Shaikh K, Alabi T (2005) "The Use of Swell Packers as a Replacement and Alternative to Cementing," Society of Petroleum Engineers, SPE Paper # 95713, *SPE Annual Technical Conference and Exhibition*, 9-12 October 2005, Dallas, Texas
- [3] Daniel L, Hertz J. "Chapter-1: Introduction" in AN Gent (ed) *Engineering With Rubber: How to Design Rubber Components*. 2nd ed. Hanser-Gardner: Publishers; 2000
- [4] Marckmann G, Verron E. Comparison of Hyperelastic Models for Rubber-Like Materials. *Rubber Chemistry and Technology*. 2006;**79**(5): 835-858
- [5] Al-Yami AS, Al-Arfaj MK, Nasr-el-Din HA, Al-Saleh SH, Al-Humaidi AS, Al-Moajil AM (2008b) "Lab Investigation of Oil Swelling Elastomers for Smart Well Completions," SPE Paper #113135, *Europec/EAGE Conference and Exhibition*, 9-12 June 2008, Rome, Italy
- [6] Qamar SZ, Pervez T, Akhtar M (2016) "Performance Evaluation of Water-Swelling and Oil-Swelling Elastomers," *Journal of Elastomers and Plastics*, 48 (6) 2016, p 535-545
- [7] Qamar SZ, Pervez T, Akhtar M, Al-Kharusi MSM. Design and Manufacture of Swell Packers: Influence of Material Behavior. *Materials and Manufacturing Processes*. 2012;**27**(7):727-732
- [8] Qamar SZ, Hiddabi SA, Pervez T, Marketz F. Mechanical Testing and Characterization of a Swelling Elastomer. *Journal of Elastomers and Plastics*. 2009;**41**(5):415-431
- [9] Al-Yami AS, Nasr-el-Din HA, Al-Humaidi AS (2008a) "Investigation of Water Swelling Elastomers: Advantages, Limitations, and Recommendations," SPE Paper # 114810, *SPE Annual Technical Conference and Exhibition*, 21-24 September 2008, Denver, Colorado, USA
- [10] Akhtar M, Qamar SZ, Pervez T, Al-Jahwari FK (2018) "Performance Analysis of Swelling Elastomer Seals," *Petroleum Science and Engineering*, 165 (2018), p 127-135
- [11] Qamar SZ, Akhtar M, Al-Kharusi MSM (2013) "Effect of Swelling Behavior on Elastomeric Materials: Experimental and Numerical Investigation," ASME-2013 International Mechanical Engineering Congress and Exhibition (IMECE-2013), 15-21 November 2013, San Diego, California
- [12] Al-Kharusi MSM, Qamar SZ, Pervez T, Akhtar M (2011) "Non-Linear Model for Evaluation of Elastomer Seals Subjected to Differential Pressure," Paper # SPE-149032, *SPE/DGS Saudi Arabia Section Technical Symposium and Exhibition*, 15-18 May 2011, Al-Khobar, Saudi Arabia
- [13] Al-Kharusi MSM, Qamar SZ, Pervez T, Akhtar M (2013) "Elastomer Seal with Frictional Contact — Analytical Solution," ASME-2013 International Mechanical Engineering Congress and Exhibition (IMECE-2013), 15-21 November 2013, San Diego, California
- [14] Gent AN, Meinecke EA. Compression, Bending, and Shear of Bonded Rubber Blocks. *Polymer Engineering and Science*. 1970;**10**(1): 48-53
- [15] Chalhoub MS, Kelly JM. Analysis of Infinite-Strip-Shaped Base Isolator with

Elastomer Bulk Compression. Journal of Engineering Mechanics. 1991;**117**(8): 1791-1805

[16] Gent AN, Lindley PB. The Compression of Bonded Rubber Blocks. Proceedings of the Institution of Mechanical Engineers. 1959;**173**(p): 111-122

[17] Yeoh OH, Pinter GA, Banks HT. Compression of Bonded Rubber Blocks. *Rubber Chemistry and Technology*, Vol. 2002;**75**:549-561

[18] Beer FP, Johnston ER, Dewolf JT, Mazurek D. Mechanics of Materials. 7th ed. McGraw-Hill: Publications; 2014